Cloud Detection in MIPAS Spectra

Dominik Kasprzyk
Exeter College
Oxford University, UK

17th April, 2002

Abstract

Cloud detection is possible in MIPAS spectra using the ratio of the average of two microwindows to gain a Cloud Index. This Cloud Index has an threshold value independent of atmosphere and altitude for cloud cover and can detect 50% cloud cover in MIPAS's field of view. Smaller percentages of cloud can be detected if considering the Cloud Index threshold is varied as a function of atmosphere and altitude. A relationship has been established between the Cloud Index and the optical thickness of cloud in the FOV. This relationship is independant of altitude and atmosphere except for equatorial atmospheres with thick cloud cover. Better accuracy can be obtained by including some dependance on atmosphere into the relationship.

1 Introduction to MIPAS

The Michelson Interferometer for Passive Atmospheric Sounding (MIPAS) is a Fourier transform spectrometer for the measurement of high-resolution emission spectra at the Earth's limb. It operates in the near to mid infrared where many of the atmospheric trace-gases playing a major role in atmospheric chemistry have important emission features.

The objectives of MIPAS are [1]:

- Simultaneous and global measurements of geophysical parameters in the middle atmosphere;
  Stratospheric chemistry: O_3, H_2O, CH_4, N_2O, NO_2 and HNO_3; and
  Climatology: Temperature, CH_4, N_2O, O_3;
- Study of chemical composition, dynamics and radiation budget of the middle atmosphere;
- Monitoring of stratospheric O_3 and CFC's.

The instrument has 5 channels (see table 1). This gives MIPAS an operational range of 685 to 2410 cm^{-1} sampled at 0.025 cm^{-1}.

The radiance detected by MIPAS is a function of presure, temperature and composition. Pressure and temperature can be retrieved from lines of CO_2, which has a fairly constant concentration of about 0.036%. Once these are known, the concentration of other gases in the atmosphere can be determined from their own emission features.

Table 1: MIPAS Spectral Bands

Channel	Wavenumber Range (cm^{-1})	Noise ($nW/cm^2sr^{-1}cm^{-1}$)
A	685 – 970	50
AB	1020 – 1170	40
B	1215 – 1500	20
C	1570 – 1750	6
D	1820 – 2410	4.2

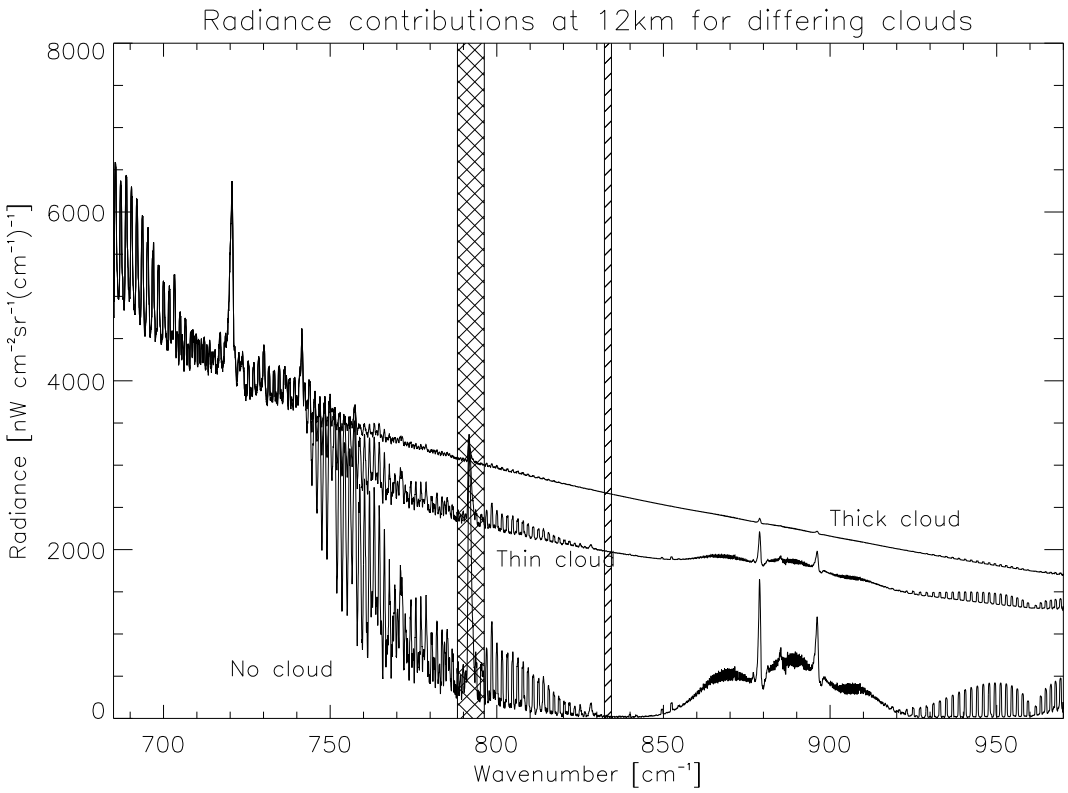

Figure 1: Various modelled specta for different amounts of cloud in the MIPAS A channel range

2 Cloud Impact on MIPAS Measurements

In the spctral range of MIPAS, cloud acts like a spectrally uniform emitter, increaseing the optical thickness of the atmosphere. Figure 1 shows 3 different spectra modelled using the Reference Foward Model (RFM) developed at Oxford University in the presence of different amounts of cloud for a mid-latitude daytime atmosphere. In the parts of the spectrum where the transmitance is high (i.e. we can see the tangent point), so from about 750 cm^{-1} in direction of increasing wavenumber, the Planck function of the cloud begins to dominate, increasing the radiance of gaseous emission lines and simultaneously merging them with the background so that they become less distinguishable from it.

MIPAS retrievals rely on the distinction between emision lines of the 'target' species and continuum-like background terms such as cloud or aerosol. With large cloud opacity, this distinction disapppears so it would be useful to identify such cloud-contaminated spectra before attempting any retieval.

3 The Cloud Index

Reinhold Sprang and John Remedios from the University of Leicester suggest that taking the ratio of the average of two certain wavenumber ranges ('microwindows') will provide a Cloud Index (CI). A value of less then a certain threshold will show whether or not there is cloud in the Field Of View (FOV). They also believe that this threshold is robust for all types of atmospheric variation. Their data is based on that from CRISTA, a grating spectrometer instrument flown on two shuttle missions. Further, they suggest this method could be extended to MIPAS, to identify cloud in data. The two ranges are shown by the shaded regions on figure 1 and are:

- Channel 1: 788.20 – 796.25
- Channel 2: 832.30 – 834.40

A CI of less then 1.8 they believe should indicate cloud[2]. By using the RFM to simulate various atmospheric conditions, we want to see:

1. Whether the CI does indeed generate some robust threshold for cloud detection and whether this threshold is 1.8, as suggested by Sprang and Remedios.
2. Whether there is some relationship between CI and a physical parameter such as cloud optical thickness in the FOV.

4 Physical basis for the Cloud Index

Monochromatic radiance through a non-scattering atmosphere can be represented by

$$R = \int_{\infty}^{0} B \frac{d\tau}{ds} ds + I_{\infty}\tau_{\infty} \tag{1}$$

where R is the radiance, B the Planck function of the emitter, s is the path through the atmosphere, $d\tau/ds$ is the weighting function of the atmosphere along the path and $I_{\infty}\tau_{\infty}$ is the radiance coming from space beyond the atmosphere[3].

Limb viewing looks at the cold background as its source, so we can neglect I_{∞}. Assuming we are also looking at parts of the atmosphere with high transmittance, so we are seeing straight to the tangent point, as shown by Figure 1. So we can consider the part of the atmosphere we are looking at as a box along our path, filled with atmospheric gases at the same temperature and conditions, with a transmitance of 1 at the entry of the box and τ at the other end. This allows us to rewrite the integral above as

$$R \approx B \int_{\tau}^{1} d\tau \tag{2}$$

and solves to

$$R = B\,(1 - \tau) \tag{3}$$

If we consider an optical depth for the atmospheric gases and for the cloud separately, and we use the relation $\tau = e^{-\chi}$, then

$$R = B\,(1 - \exp\,(-\chi - \chi_c)) \tag{4}$$

where B is the Planck function, χ is the optical depth of the atmospheric gases and χ_c is the optical depth of the cloud.

If we have two microwindows that are close in wavelength, R_1 and R_2, we can assume χ_c is constant with wavelegth (i.e. same for both microwindows) and $B_1 \approx B_2$.

So, if we take the ratio of the two microwindow radiances (the CI) we get:

$$\mathrm{CI} = \frac{\mathrm{R}_1}{\mathrm{R}_2} \approx \frac{1 - \exp\,(-\chi_1)\,.\exp\,(-\chi_c)}{1 - \exp\,(-\chi_2)\,.\exp\,(-\chi_c)} \tag{5}$$

where χ_1 and χ_2 are assumed to be known, so χ_c is the only variable. This implies some constant relationship between CI and χ_c, while χ_1 and χ_2 remain constant.

5 A Threshold Value

5.1 A Suitable Test

For there to exist a suitable threshold in cloud determination in MIPAS spectra, this threshold must be able to distinguish cloudy spectra independent of altitude and atmospheric conditions. So, if the CI was indeed a good indicator of cloud, with a robust threshold, then any plot of CI against altitude should have some fairly sharp differences between cloudy CIs and non-cloudy CIs.

Given that MIPAS's Field Of View (FOV) is 3km high, we cannot always expect a very sharp divide between non-cloudy CIs and cloudy CIs. The question then arises, what happens when there is cloud only partially in the FOV? This is dealt with in the next section, but will be of interest here because of the altitude plot of the CI.

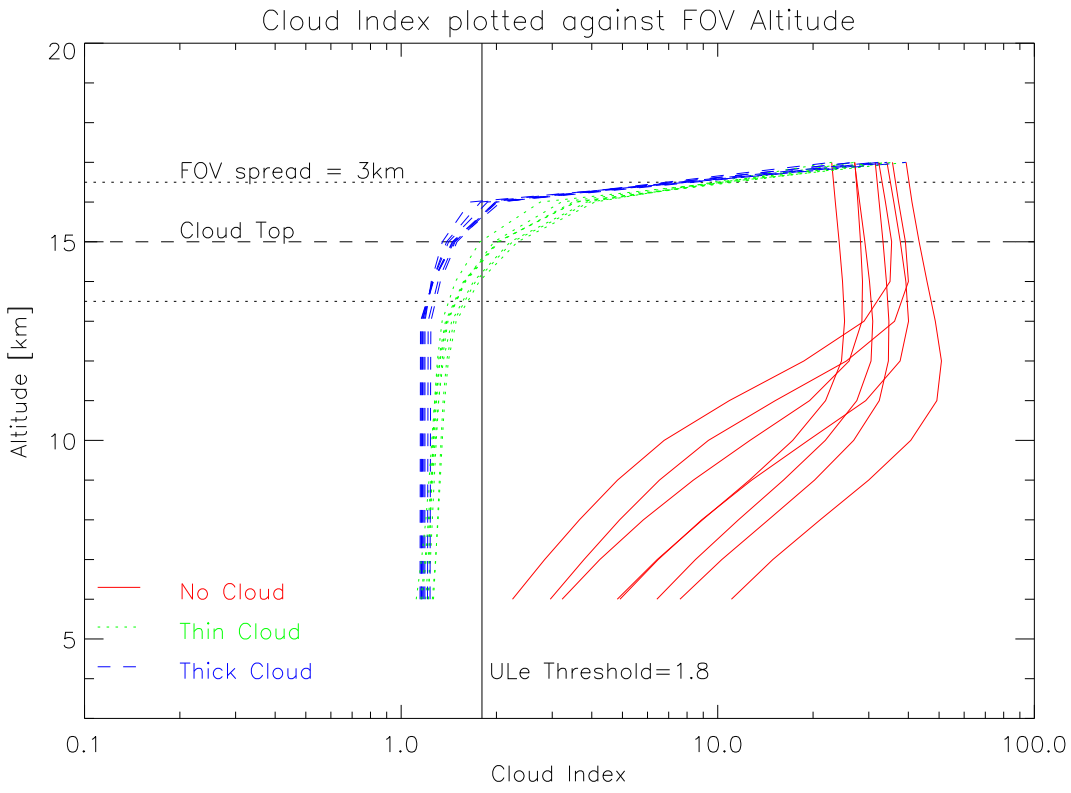

Figure 2: Cloud Index plotted against altitude for the various atmospheres. Note the threshold line.

5.2 Plotting the Cloud Index

The RFM was used to simulate radiance and transmittance data for various types of cloud in 8 differing atmospheres for the two microwindows. The atmospheres were: mid-latitude, equatorial, polar summer and polar winter and the same again but with all parameters such as temperature and water vapour increased by a typical climatological variability 1σ. The cloud was simulated with an uniform cross-section up to a height of 15km and the following cases were simulated:

1. None (cloud optical depth 0)
2. Thin (cloud optical depth ≈ 1)
3. Thick (cloud optical depth 10)

The RFM was run for various tangent heights ranging through and above the cloud for the different atmospheres and cloud covers. Once data were collected the radiances were averaged over the two individual microwindows and these average radiances were then averaged over the FOV of MIPAS, giving the radiance at each height as MIPAS would see it. The CI could then be worked out from the radiance figures for each microchannel:

$$\bar{R}_i = \frac{\int_{mw_i} \int_{FOV} R(\tilde{\nu}, \phi)\, d\tilde{\nu} d\phi}{\int_{mw_i} d\tilde{\nu} \int_{FOV} d\phi} \tag{6}$$

where $\tilde{\nu}$ =wavenumber and ϕ =solid angle.

5.3 Cloud Index behaviour over altitudes

Figure 2 shows eight different lines for each cloudiness, one for each atmosphere considered. Note the ULe suggested threshold marked and the grouping of all cloudy data under the cloud top height in a small CI

range while CIs near the cloud top change gradually back to cloudless figures. Also note how the ULe suggested threshold corresponds very well to the cloud top height (i.e. when the FOV is half filled by cloud) and how all the cloudy data is below it while the cloudless data is entirely above it.

The grouping of data in such a small range is good indication that there is a threshold CI for which we can say there is (or isn't) any cloud in the spectrum. It can be seen that the ULe threshold is a good choice, being as high as possible before being confused with cloudless data. The cloudy data ranges from equatorial $+1\sigma$ nearest the CI threshold to polar winter with the largest CI and the rest spreading evenly in between, which is reassuring in picking 1.8 as a threshold because it suggests that temperature or humidity influences the CI even for cloud free cases and 1.8 allows some tolerance. In the region of the cloud top height, however, the CI changes rapidly and it is hard to say what threshold value would be most acceptable. Given that these CI values are caused by the cloud partially filling the FOV, then further examination about the behaviour of the CI in partial FOVs should yield more light on the matter.

6 Dependence of the CI on partial cloud cover

The MIPAS FOV is a 3×30 km rectangle. While there may be cloud in the FOV, in reality, often the cloud may not fully fill the box, in which case it is interesting to see how this affects the CI. If we imagine rectangular cloud fractionally filling the box then there are two conceivable ways this can happen, horizontally, where the cloud lies across the whole FOV or vertically, where one can always see through, so only partial amounts of the FOV are obscured. To give physical examples of such cloud, stratus cloud is thick horizontal cloud, cirrus thin horizontal cloud, cumulus is thick vertical cloud and cirrocumulus is thin broken horizontal cloud. Figure 3 shows the various FOV convolutions that were performed, with transmittance values for the case of 10km. Note that because data for three cloud types was obtained (none, thin and thick) that means three convolutions could be performed, no cloud with thin and thick and thin cloud with thick cloud and all the convolutions that were performed were multiples of 25% due to there being 4 points of data used to integrate each FOV either vertically or horizontally. Less common situations of thicker cloud overlying thinner cloud are not considered nor are both horizontal and vertical combinations together.

6.1 Vertically mixed cloud

This was simulated from radiance data by combining clear and the appropriate cloudy data to create the layering shown in figure 3. This is in effect the same as simulating a cloud top at various heights and obtaining radiances around it. One CI was obtained for every atmosphere, convolution, altitude and percentage cover and this was then plotted against altitude. Figure 4 shows the combination of no cloud with thick cloud, which shows a clear grouping of all the cloudy CIs away from the non-cloudy cases, the only exception being at very low altitudes. Furthermore, it shows that the Sprang and Remedios threshold will catch cases of 50% cloud or more, probably slightly better (although not 25%). In the case of thin cloud (figure 5), this case only becomes as good as 50%. However, any combinations of thin and thick cloud fall lower then the threshold (figure 6), so a fully filled FOV will be detected by the CI anyway. In the case of better cloud detection at 9km or greater it might not be unreasonable to use a larger threshold if required, 3.4 being adequate for this threshold.

Note the lack of points for various percentages around the marked cloud top. This is because the same cloud top was used as the last plot which limits the combinations that can be performed as the cloudy and non-cloudy pencil beams used to generate the FOV become the same above the cloud.

6.2 Horizontally mixed cloud

For this case, the end FOV radiances were taken for each altitude and with an appropriate weighting for the percentage and combined with another cloud type's FOV radiances (again weighted) to get the CI. Like with the vertically mixed case, the CI was plotted against altitude for all the different atmospheres and the convolutions are shown in figures 7–9. Comparing figure 7 with figure 4, it is possible to see that it is very similar with the one notable difference being that the cloudy points do not converge on each around the cloud top. Also, the threshold is slightly less sensitive. Again we see the threshold indicating whether there is 50% cloud or more and just like in the vertically mixed case, the same is true for the thin cloud while the convolution of thin cloud with thick cloud again falls completely below the threshold. Again, should a more sensitive cloud determination be needed above 9km, the threshold can be raised to 3.4 to rule out all cloud. Note the points marked 'other' on this convolution. They are where the cloud top causes a

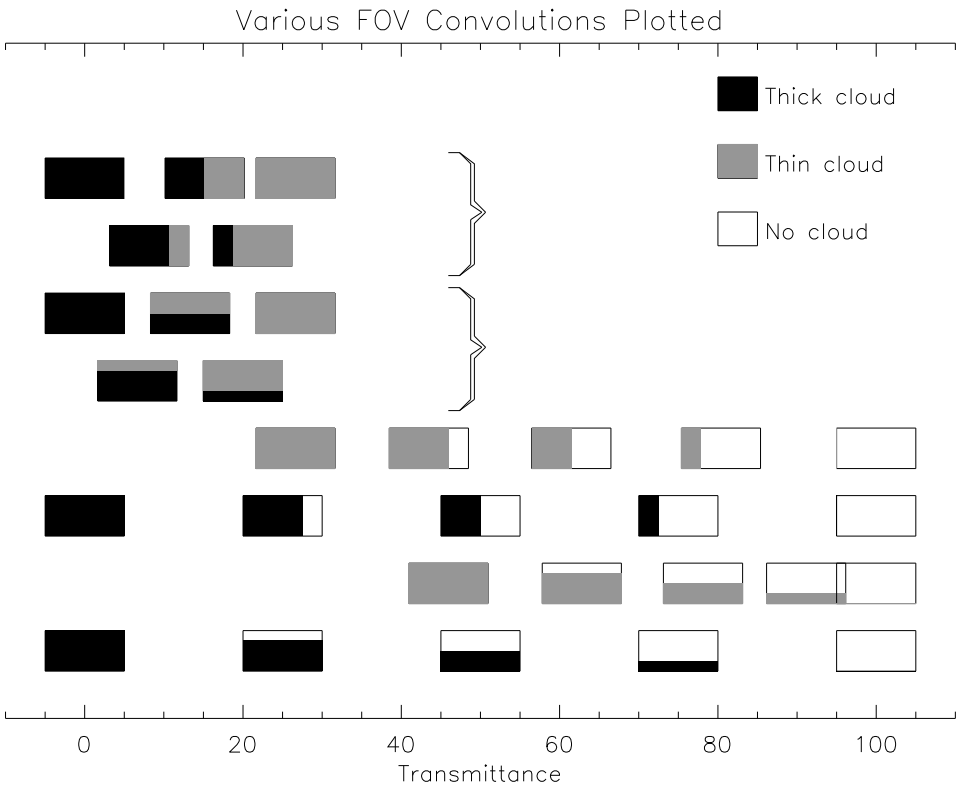

Figure 3: Various simulated FOV

vertical convolution in addition to the horizontal one being performed. They are example points of when both convolutions apply simultaneously and are included for interest.

7 Relating the Optical Thickness to the Cloud Index

As all the data has been simulated using the RFM, the transmittance values for the clouds simulated at varying altitudes are known. Using these transmittance values, it would be useful to link the rather arbitrary CI values to some physically meaningful value.

7.1 Transmittance against CI

The plot of transmittance against CI is shown in figure 10 and from that it can be seen that there is a good curve, apart from lines (peaks) centred on multiples of 0.25 transmittance.

7.2 Analysis

As all the points plotted in figure 10 are functions of atmosphere, altitude, convolution type, FOV coverage and method of mixture (horizontal or vertical), it was decided to see if any of these factors was soley responsible for the peaks in the graph or had any correlation with the curve.

Given that the original model required constant values of optical thickness for the two channels, it is quite likely that these peaks or some form of correlation would be due to pressure changes between the altitudes. However, from figure 10 it is impossible to see any relationship between the points and the altitude.

It was discovered that the peaks were composed soley of points belonging to the thick/clear combination and that the majority of points in these peaks belonged to the equatorial and equatorial $+1\sigma$ (equatorial var) atmospheres. Figure 11 shows the transmittance plotted against CI again but this time with the atmospheric type highlighted. It is possible to see a that each atmosphere has the same curve shape but with them spread in the CI axis. This suggests that atmosphere is a more important factor then altitude in calculating a more

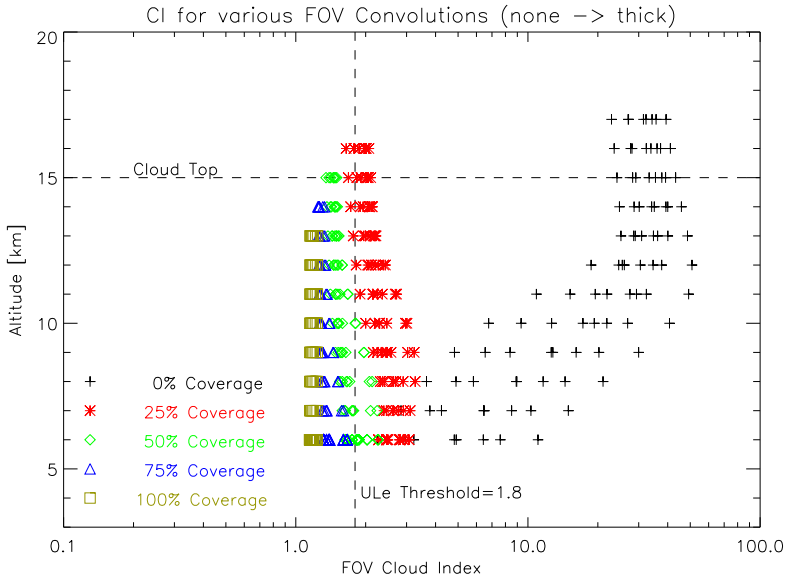

Figure 4: None – Thick cloud convolution for vertically mixed cloud

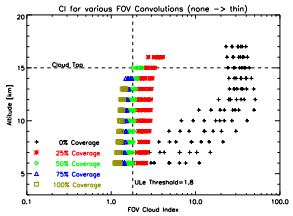

Figure 5: None – Thin

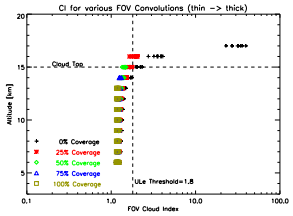

Figure 6: Thin – Thick

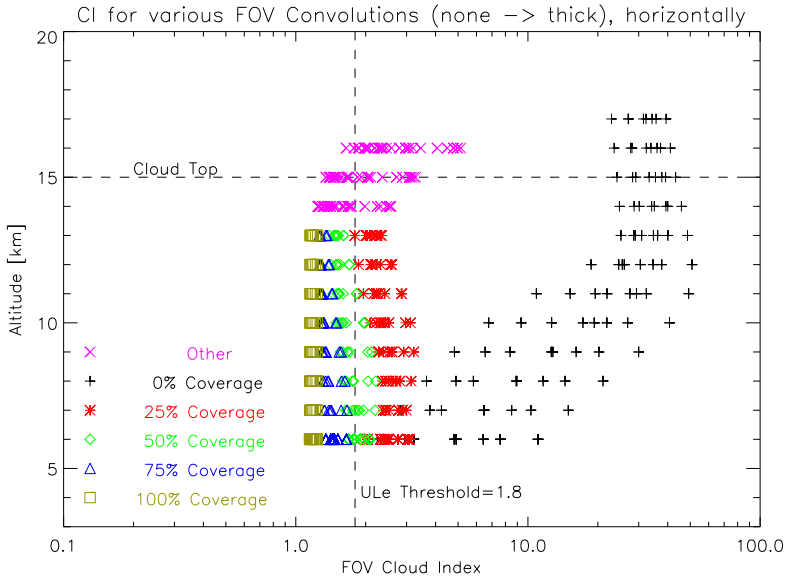

Figure 7: None – Thick cloud convolution for horizontally mixed cloud

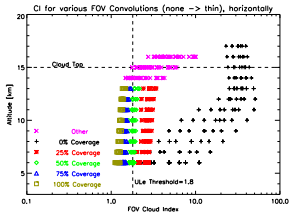

Figure 8: None – Thin

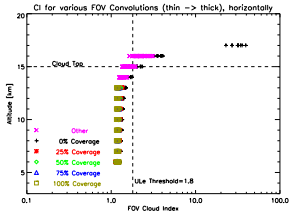

Figure 9: Thin – Thick

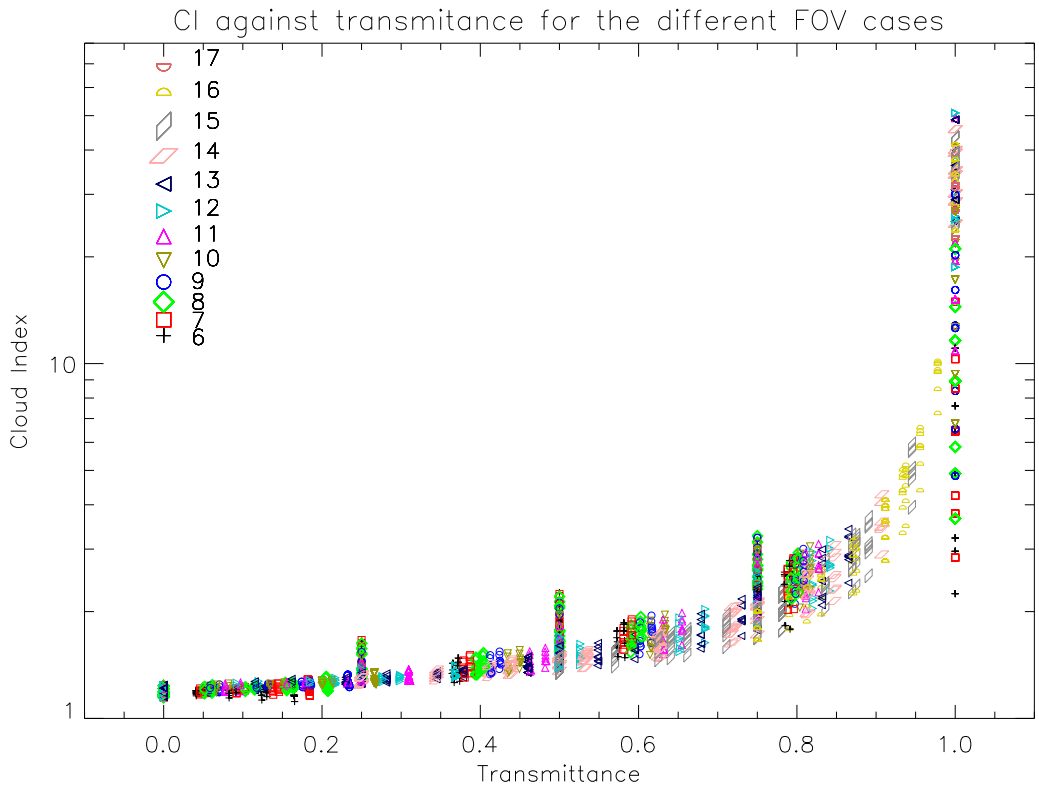

Figure 10: Transmittance plotted against the CI. Notice the quite good curve shape and the large groupings at multiples of 0.25 transmittance corresponding to thick/clear combinations. The colour/symbol indicates altitude and notice how there is no correlation between altitude and the curve.

precise value of the transmittance from the CI, although the spread of atmospheres ranges from polar summer through to polar winter which does not immediately suggest what atmospheric variable may be the cause of the spread and what atmospheric parameter should be taken into account to produce a better fit of some equation to the data.

In relation to the peaks, it also shows the composition of the peaks, the points with the largest CIs belonging to the two equatorial atmospheres exclusively. Tracing some of these outlying points for the equatorial atmospheres by replotting the FOV combinations with atmosphere highlighted it is possible to see that instead the CI decreasing between the none and thin combination (figures 5 and 8) and the none and thick combination (figures 4 and 7), the equatorial points actually increase in CI with thinner cloud. These points are in fact the ones that can be seen with the highest values of CI in every FOV percentage in figures 4 and 7 for the lower altitudes.

Figure 12 shows a simulated spectrum for the equatorial $+1\sigma$ atmosphere. Normally, line emissions are weak in these microwindows so any additional opacity increases the radiance. However, for hot, moist, tropical atmospheres, even in thin cloud cases, the lower (hotter) line emissions and cloud blackbody radiation that can be seen with higher transmittance are very strong, enough that adding colder cloud at higher (colder) altitudes leads to a net reduction in radiance and the higher CI value.

7.3 Fitting the Line

Equation 5 shows the expected relationship between the CI and the optical thickness. If we convert this to transmittance using the relationship $\tau = e^{\chi}$ we get:

$$\mathrm{CI} = \frac{1 - \tau_1 \tau_c}{1 - \tau_2 \tau_C} \tag{7}$$

This equation relies on constant τ_1 and τ_2 to solve for τ_c, however, we have results for different altitudes. But, figure 10, when highlighted according to altitude, showed no clear altitude dependance anywhere in the

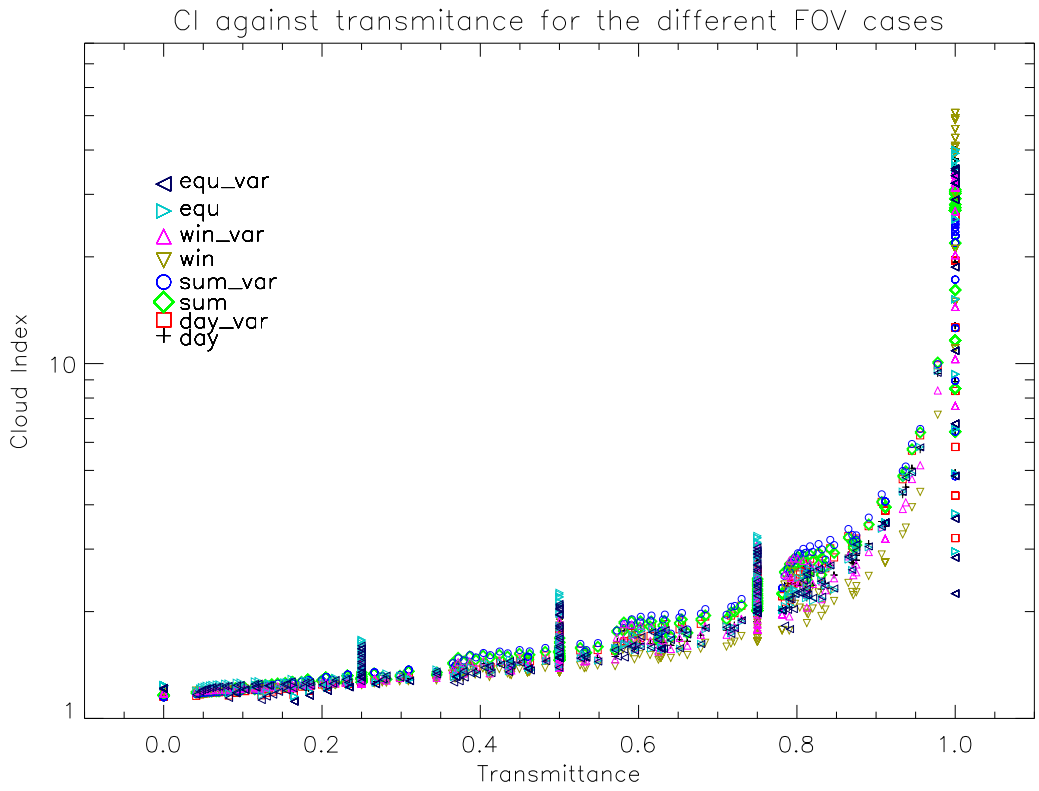

Figure 11: Transmittance plotted against the CI again with the different atmospheres highlighted. Note, $+1\sigma$ atmospheres are those with _var appended.

plot, so it was decided to ignore this in fitting the curve. To fit the curve, the IDL procedure CURVEFIT was used. This works by minimising the χ^2 value for some function and two sets of data supplied to it by minimising the function's coefficients. This requires a function to fit to, some starting values for the coefficients and the partial derivatives of the coefficients. So, from equation 7, after we rearrange it to get τ in terms of the CI (which is more sensible if we want to know the transmittance from the CI), we see the following curve lending itself for fitting:

$$\tau = \frac{a_0 - a_1 \mathrm{CI}}{a_2 - a_3 \mathrm{CI}} \tag{8}$$

where a_0 to a_3 are all coefficients adjusted by the fitting program.

The CURVEFIT program was run on the data with the above function and figure 13 shows the curve with the function obtained on it along with error values for three transmittance regimes. The coefficients, regimes and their error values are shown in tables 2 and 3.

Table 2: Coefficients of the line fit

Coefficient	*Value*
a_0	1.4292543
a_1	1.2301300
a_2	0.93818794
a_3	1.1922730

Table 3: Errors for fit of Ci against transmittance

CI Regime	*Regime*	*Error*
$1.16 \leq \mathrm{CI} < 1.37$	$0 \leq \tau_c < 0.37$	0.077
$1.37 \leq \mathrm{CI} < 3.72$	$0.37 \leq \tau_c < 0.90$	0.071
$3.72 \leq \mathrm{CI} < 12.97$	$0.90 \leq \tau_c < 1$	0.027
$\mathrm{CI} > 1$	$\tau_c > 1$	0.037
CI all values	τ_c all values	0.069

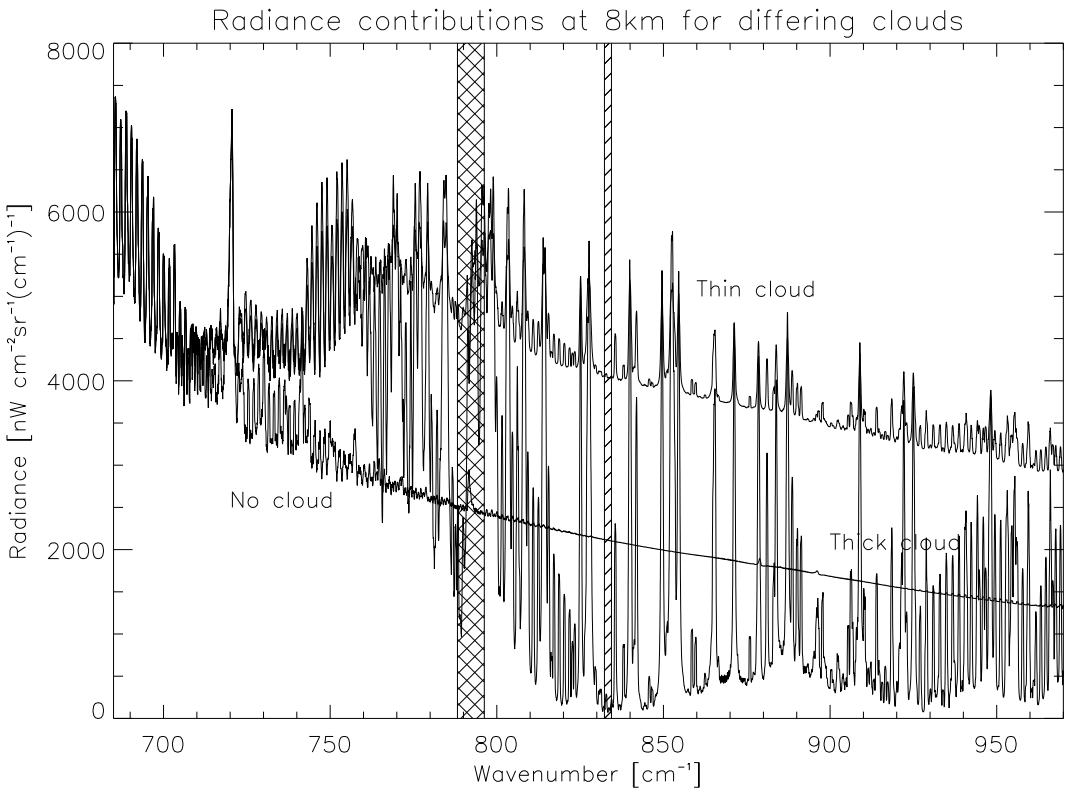

Figure 12: Simulated MIPAS A channel spectrum for the three cloud covers at 8km for an equatorial $+1\sigma$ atmosphere

8 Conclusion

The CI does provide a robust threshold for the detection of cloud in MIPAS spectra. It is possible to distinguish about 50% cloud cover independent of altitude, atmosphere and the way in which the cloud fills the FOV by using the ULe proposed threshold of 1.8. It is possible to distinguish less than 25% cloudy spectra for any atmosphere using a higher value using a threshold of 3.4 for 8km or above. Beyond these criteria, the CI must be considered a function of altitude, atmosphere and cloud cover for more sensitive cloud detection in MIPAS spectra.

There is a relationship between the CI and the transmittance. It is possible to determine the transmittance of a cloud in a spectrum to some degree of accuracy from a CI. This relationship breaks down in equatorial atmospheres for thick cloud only, where thick cloud is defined as a transmittance of zero at any altitude point. The curve can be made more accurate by considering atmospheric parameters.

9 Further Work

Of direct consequence from this study, it would be worth extending the physical basis of the CI to try and model the effect of atmospheric parameters on the the CI and to then try to extend this to refine the fitted equation between the transmittance and the CI so that it can be made more accurate.

Additional aims of further interest include:

- Whether a better combination of the two wavenumber ranges can be found for determining the optical thickness of the cloud than a simple ratio.
- Whether there exist better channels then those suggested by Sprang and Remedios.

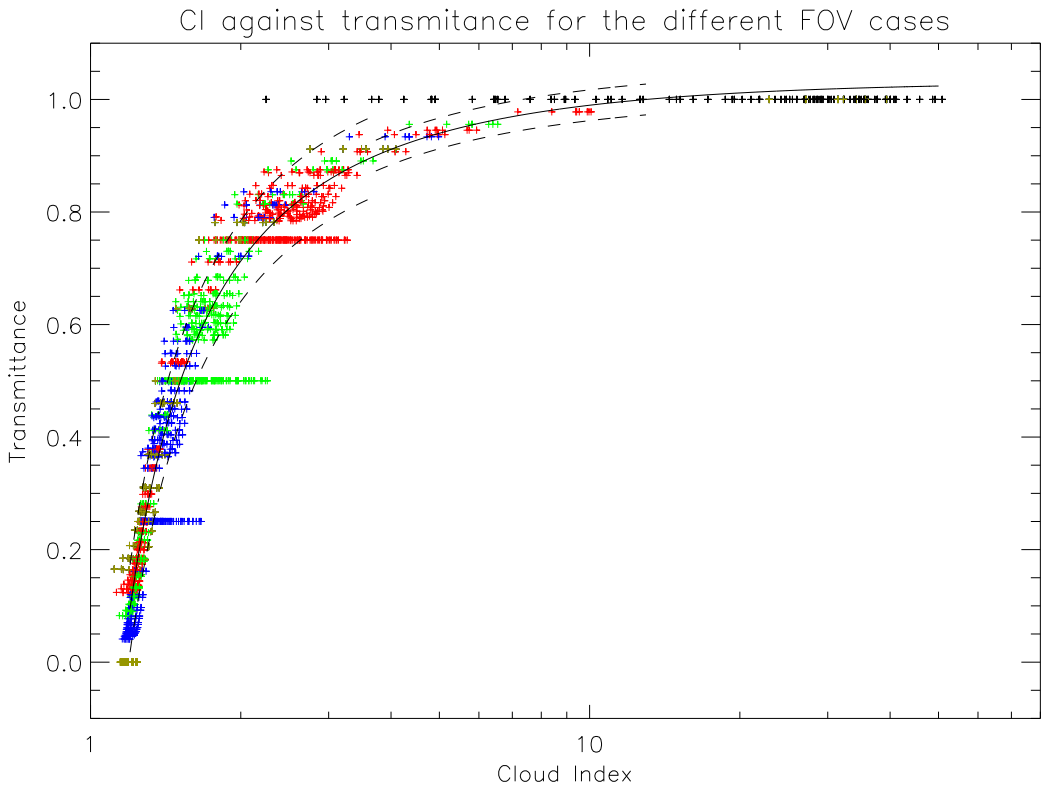

Figure 13: The CI plotted against transmittance. Error lines of $\pm\chi$ are shown for three regimes.

10 Evaluation

Much of the data is a function of a great many parameters which lends itself to storage in mass multi-dimensional arrays. In this sense the use of IDL was very helpful because of its support of array handling, its storage of the variables publically allowing different program components to be writen to do different things (e.g. read in the data in one module, process it in another and plot in a third) which greatly reduces work time and the ability to extract data from these arrays to plot them quickly and I would recommend any further work to be done in IDL or similar language.

In writing the input and analysis parts of the programs used to analyse this data, I found it very helpful to make sure that the programs got their input and calculation parameters for height and atmosphere directly out of arrays specifying them. This meant the number of altitudes and atmospheres used could be increased arbitrarily and the programs would handle it and I believe this to be worth the extra time it took to write in variables and calculate them from these initial arrays.

References

[1] ESA, Envisat, *MIPAS Introduction* (Webpage 2002) http://envisat.esa.int/instruments/mipas/index.html

[2] Remedios and Sprang, *Presentation at MIPAS Study Progress Meeting (PM 18)* in IROE-CNR Florence, ref PO-MN-ESA-GS-1310, 01 Feb 2002

[3] Dudhia A, Satellite Remote Sensing: Temperature Soundings in the *Encyclopedia of Atmospheric Sciences*, to be published by Academic Press, 2002